Supplementary Materials

SPdKS analysis of ultra-low velocity zones beneath the western Pacific

Kevin J. Jensen, Michael S. Thorne and Sebastian Rost

The supplementary material included here is organized in the following sections.

S1. Summary of past studies in this region

S2. Events used in this study

S3. ULVZ models calculated for this study

S4. Distance profiles of all data

S5. Model Comparisons

S1. Summary of past studies in this region

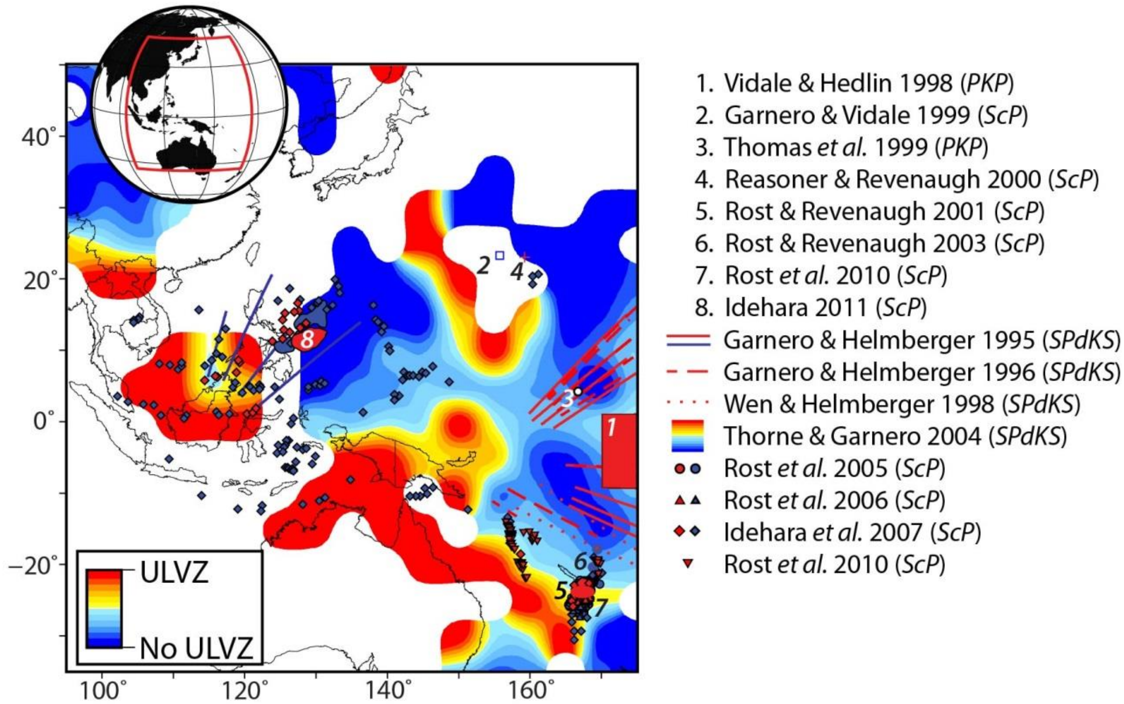

Figure S1. Summary of past studies that have investigated our study region for ULVZ presence. In all cases red colors indicates that the study determined likely ULVZ presence, whereas blue colors indicate that no ULVZ was found.

References for Figure S1.

Garnero, E. J., and D. V. Helmberger (1995), A very slow basal layer underlying large-scale low-velocity anomalies in the lower mantle beneath the Pacific: evidence from core phases, *Phys. Earth Planet. Inter.*, *91*, 161-176.

Garnero, E. J., and D. V. Helmberger (1996), Seismic detection of a thin laterally varying boundary layer at the base of the mantle beneath the central-Pacific, *Geophys. Res. Lett.*, *23*(9), 977-980.

Garnero, E. J., and J. E. Vidale (1999), ScP; a probe of ultralow velocity zones at the base of the mantle, *Geophys. Res. Lett.*, *26*(3), 377-380.

Idehara, K. (2011), Structural heterogeneity of an ultra-low-velocity zone beneath the Philippine Islands: Implications for core–mantle chemical interactions induced by massive partial melting at the bottom of the mantle, *Phys. Earth Planet. Inter.*, *184*, 80-90, doi: 10.1016/j.pepi.2010.10.014.

Idehara, K., A. Yamada, and D. Zhao (2007), Seismological constraints on the ultralow velocity zones in the lowermost mantle from core-reflected waves, *Phys. Earth Planet. Inter.*, *165*, 25-46, doi: 10.1016/j.pepi.2007.07.005.

Reasoner, C., and J. Revenaugh (2000), ScP constraints on ultralow-velocity zone density and gradient thickness beneath the Pacific, *J. Geophys. Res.*, *105*(B12), 28173-28182.

Rost, S., and J. Revenaugh (2001), Seismic Detection of Rigid Zones at the Top of the Core, *Science*, *294*, 1911-1914.

Rost, S., and J. Revenaugh (2003), Small-scale ultralow-velocity zone structure imaged by ScP, *J. Geophys. Res.*, *108*(B1), doi: 10.1029/2001JB001627.

Rost, S., E. J. Garnero, and Q. Williams (2006), Fine-scale ultralow-velocity zone structure from high-frequency seismic array data, *J. Geophys. Res.*, *111*(B09310), doi: 10.1029/2005JB004088.

Rost, S., E. J. Garnero, and W. Stefan (2010), Thin and intermittent ultralow-velocity zones, *J. Geophys. Res.*, *115*(B06312), doi: 10.1029/2009JB006981.

Rost, S., E. J. Garnero, Q. Williams, and M. Manga (2005), Seismological constraints on a possible plume root at the core-mantle boundary, *Nature*, *435*, 666-669, doi: 10.1038/nature03620.

Thomas, C., M. Weber, C. W. Wicks, and F. Scherbaum (1999), Small scatterers in the lower mantle observed at German broadband arrays, *J. Geophys. Res.*, *104*(B7), 15073-15088.

Thorne, M. S., and E. J. Garnero (2004), Inferences on ultralow-velocity zone structure from a global analysis of SPdKS waves, *J. Geophys. Res.*, *109*, doi: 10.1029/2004JB003010.

Vidale, J. E., and M. A. H. Hedlin (1998), Evidence for partial melt at the core-mantle boundary north of Tonga from the strong scattering of seismic waves, *Nature*, *391*, 682-685.

Wen, L., and D. V. Helmberger (1998), A two-dimensional P-SV hybrid method and its application to modeling localized structures near the core-mantle boundary, *J. Geophys. Res.*, *103*(B8), 17901-17918.

S2. Events used in this study

Table S1. Earthquakes used in this study.

Event	Date	Latitude, deg	Longitude, deg	Depth, km	Mw
1	18 MAY, 1993	19.8	122.5	214	6.1
2	7 AUG, 1993	-23.9	179.8	555	6
3	25 DEC, 1995	-6.9	129.2	150	6.2
4	28 FEB, 1996	1.7	126.1	103	6.1
5	5 NOV, 1996	-31.2	180	369	5.9
6	1 DEC, 1996	-30.5	-179.7	356	6.1
7	21 MAR, 1997	-31.2	179.6	449	6.3
8	23 APR, 1997	14	144.9	101	6.2
9	3 MAY, 1997	-31.8	-179.4	108	6.6
10	4 SEP, 1997	-26.6	178.3	625	6.3
11	23 MAY, 1998	8.1	123.7	658	5.9
12	9 JUL, 1998	-30.5	-179	130	6.2
13	27 DEC, 1998	-21.6	-176.4	144	6.1
14	9 APR, 1999	-26.4	178.2	621	6.2
15	3 MAR, 2000	-7.3	128.5	142	6.4
16	10 JUL, 2000	-4.5	103.8	105	5.8
17	15 JUL, 2000	-7	128.9	218	5.9
18	16 FEB, 2001	-7.2	117.5	521	5.9
19	19 MAR, 2002	-6.5	129.9	148	6.1
20	5 MAY, 2003	0.2	127.4	124	5.9
21	25 JUL, 2004	-2.4	104	582	6.8
22	5 FEB, 2005	5.3	123.3	525	6.4
23	15 OCT, 2005	25.3	123.4	183	6.2
24	15 JAN, 2006	-7.8	122.6	265	6
25	26 FEB, 2006	-23.6	-180	535	5.9
26	15 JUL, 2006	-4.5	126.2	368	5.8
27	14 NOV, 2006	-6.4	128	352	6.1
28	23 JUL, 2007	-4.5	149.9	572	5.9
29	25 SEP, 2007	-31	180	417	6.2
30	29 APR, 2008	-6.1	127.5	405	5.9
31	26 APR, 2009	-30.3	-178.6	132	6.1
32	4 OCT, 2009	6.7	123.4	620	6.4
33	24 OCT, 2009	-6.1	130.4	130	6.7
34	22 NOV, 2009	-31.6	179.5	436	6.2
35	16 MAY, 2010	0.5	124.7	123	5.8
36	17 JUN, 2010	-33.2	179.7	170	6.0
37	21 JUL, 2010	3.0	128.2	100	6.0
38	23 JUL, 2010	6.5	123.5	586	6.9
39	24 JUL, 2010	6.2	123.5	553	5.9
40	29 JUL, 2010	6.5	123.2	627	6.1

S3. ULVZ models calculated for this study

Table S2. ULVZ models computed for SPdKS analysis.

δV_S (%)	**δV_P (%)**	**$\delta\rho$ (%)**	***h* (km)**	**Length (deg)**	**Length (km on CMB)**	**Edge* (deg)**
-15	-5	+10	10, 15, 20, 30	1.5	91	10, 11.5, 13, 14.5, 16, 17.5, 19
-15	-5	+10	5, 10, 15, 20, 30	3	182	8.5, 10, 11.5, 13, 14.5, 16, 17.5, 19
-15	-5	+10	10, 15, 20	6	364	5.5, 7, 8.5, 10, 11.5, 13, 14.5, 16, 17.5, 19
-15	-5	+10	7.5, 10, 15, 20, 25	12	728	1, 2.5, 4, 5.5, 7, 8.5, 10, 11.5, 13, 14.5, 16, 17.5, 19
-30	-10	+10	10, 15, 20, 30	1.5	91	10, 11.5, 13, 14.5, 16, 17.5, 19
-30	-10	+10	5, 7.5, 10, 12.5, 15, 20, 30	3	182	8.5, 10, 11.5, 13, 14.5, 16, 17.5, 19
-30	-10	+10	7.5, 10, 15, 20, 30	6	364	5.5, 7, 8.5, 10, 11.5, 13, 14.5, 16, 17.5, 19
-30	-10	+10	7.5, 10, 15	12	728	1, 2.5, 4, 5.5, 7, 8.5, 10, 11.5, 13, 14.5, 16, 17.5, 19
-45	-15	+10	10, 15, 20, 30	1.5	91	10, 11.5, 13, 14.5, 16, 17.5, 19
-45	-15	+10	5, 7.5, 10, 12.5, 15, 20, 30	3	182	8.5, 10, 11.5, 13, 14.5, 16, 17.5, 19
-45	-15	+10	5, 7.5, 10, 15, 20	6	364	5.5, 7, 8.5, 10, 11.5, 13, 14.5, 16, 17.5, 19
-45	-15	+10	5, 7.5, 10, 15	12	728	1, 2.5, 4, 5.5, 7, 8.5, 10, 11.5, 13, 14.5, 16, 17.5, 19

S4. Distance Profiles

Distance profiles are provided for each of the four study regions examined. In each figure the left hand column shows original data (light gray traces) and stacks (black traces) in 1° epicentral distance bins. All data are radial component displacement traces aligned and normalized to unity on the SKS arrival. Right hand column shows data stacks (black traces) overlain on PREM synthetics.

Coral Sea Region

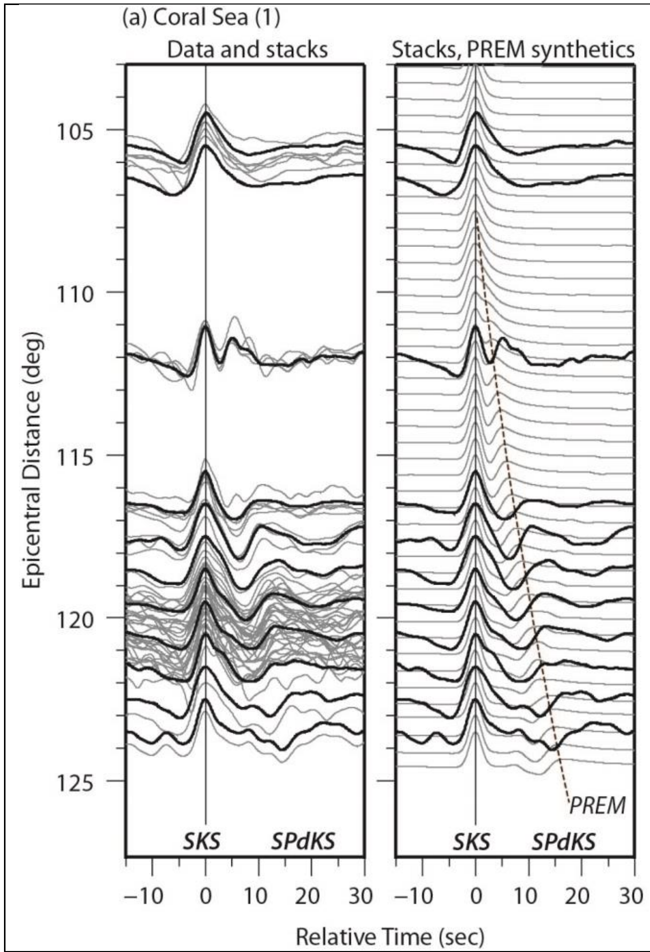

Coral Sea. Bin 1.

South Philippine Sea Region

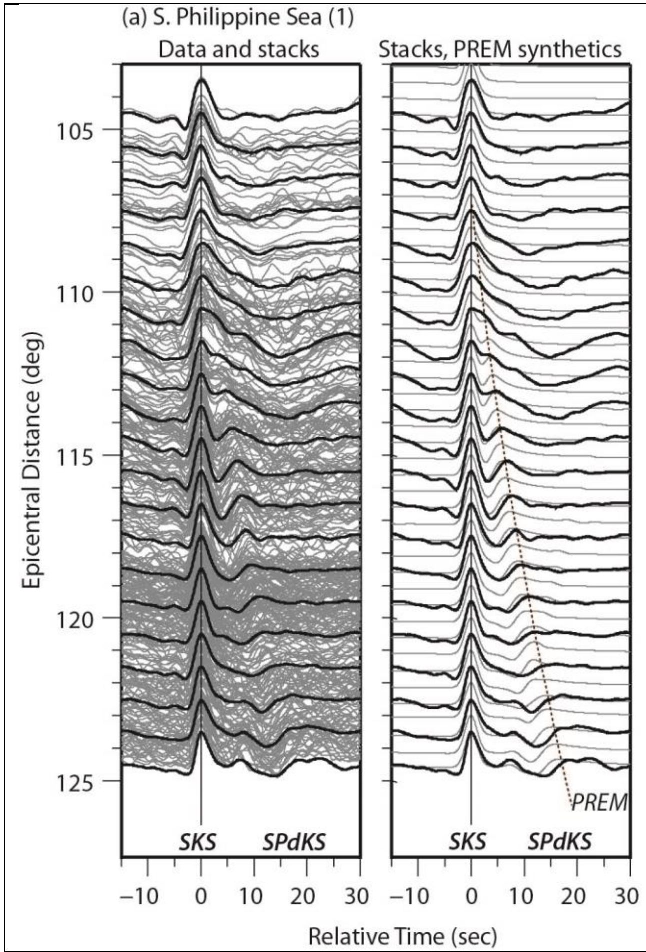

South Philippine Sea. Bin 1.

North Philippine Sea Region

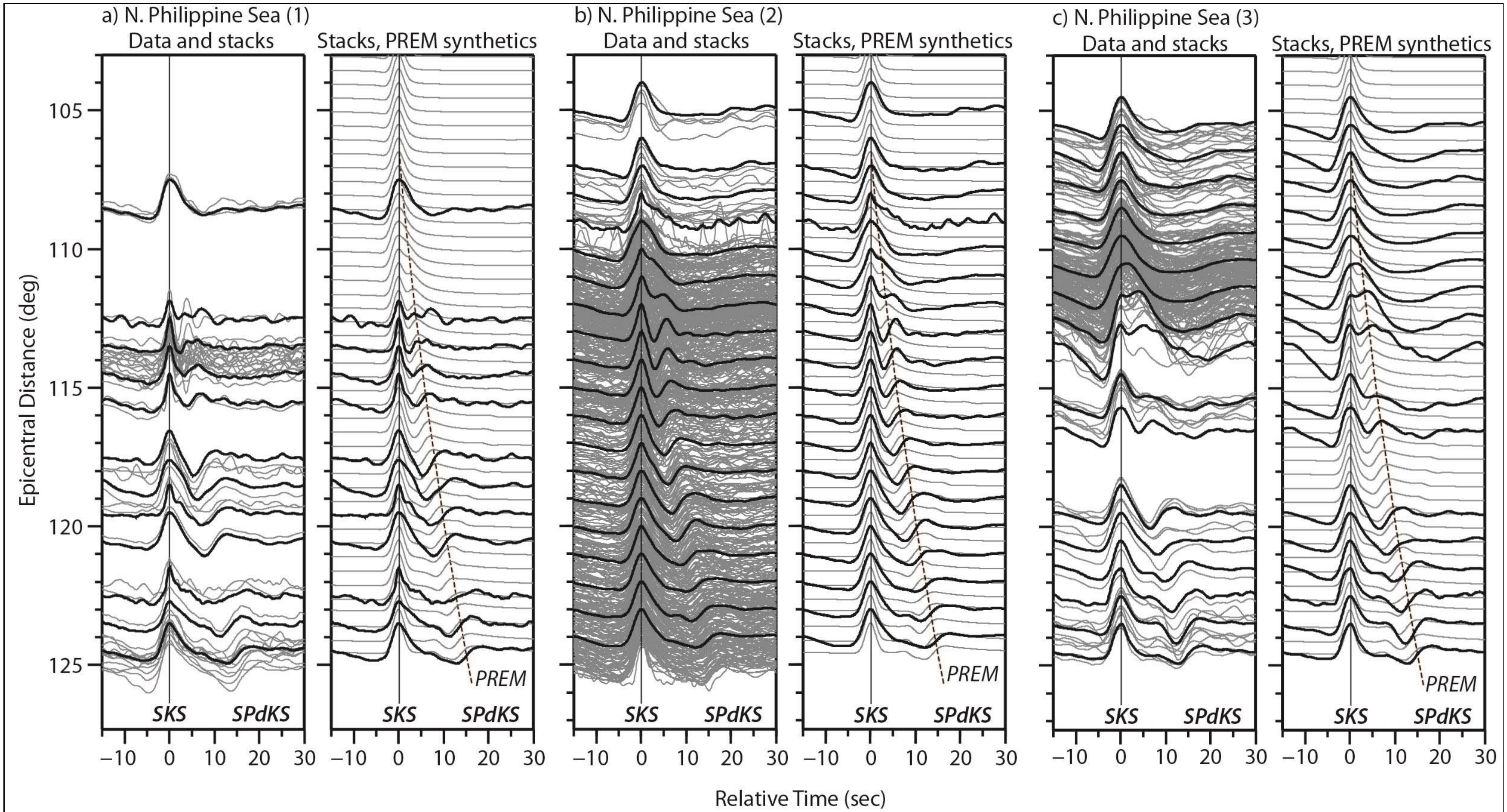

North Philippine Sea. Bins 1, 2, and 3.

South China Sea Region

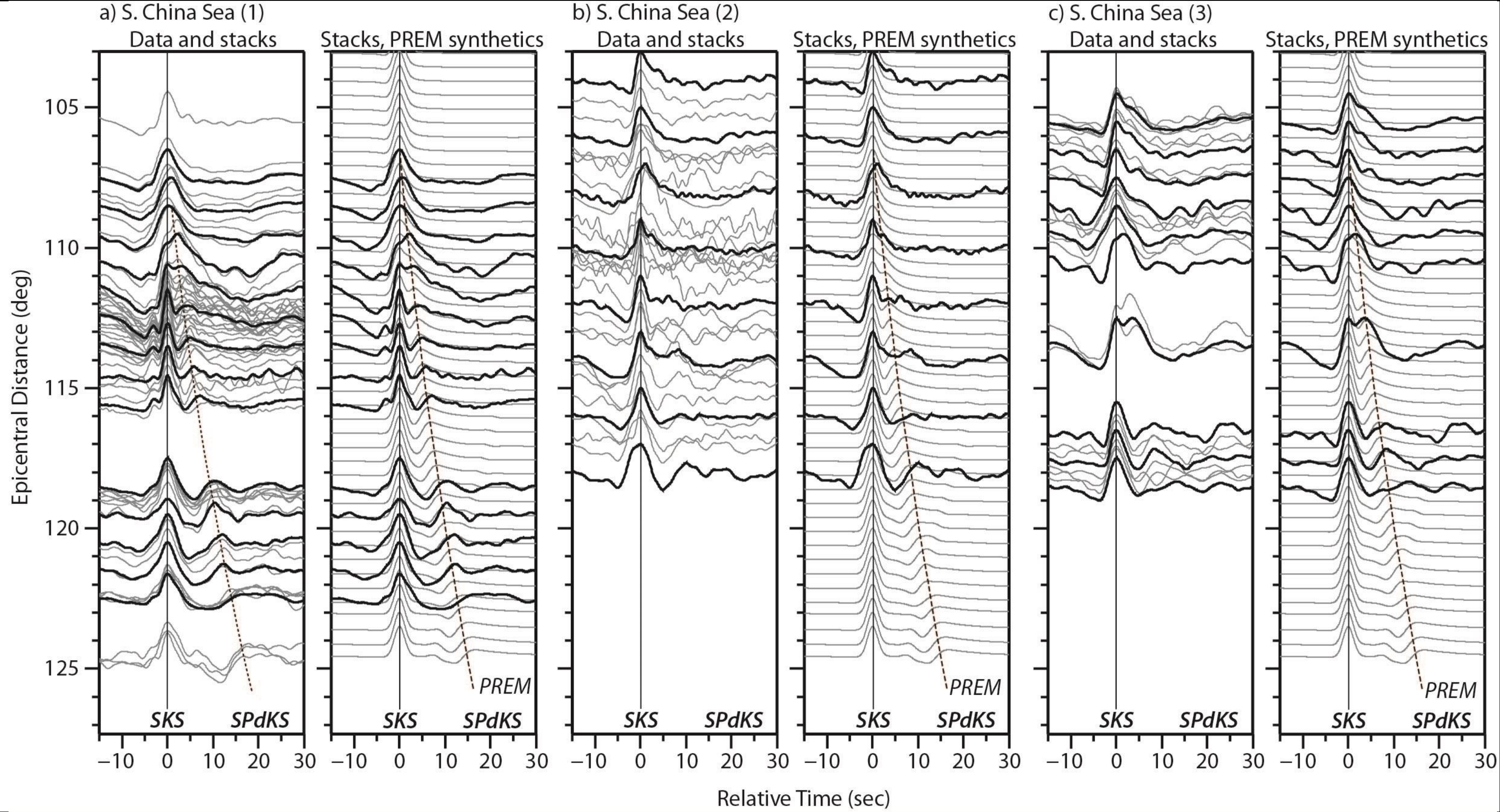

South China Sea. Bins 1, 2, and 3.

S5. Model Comparisons

The following figures show the results of 517 ULVZ models compared by the mean of data stack CCCs (right-hand panel). The figures are separated into twelve plots based on seismic velocity decrease and length of the ULVZ in degrees. The top labels (S#/P#) represent the decrease in ULVZ V_S and V_P respectively. ULVZ thickness is organized along the y-axis and ULVZ Δ_{edge} position is given along the x-axis. The top 5 models are marked with a star (red=best-fit, orange=2nd, green=3rd, cyan=4th, gray=5th). The PREM model is in the bottom left corner of the top left box. Left-hand plot) shows the percent confidence of a Welch's t-test when all the models are compared to the model with the highest mean.

Coral Sea Region

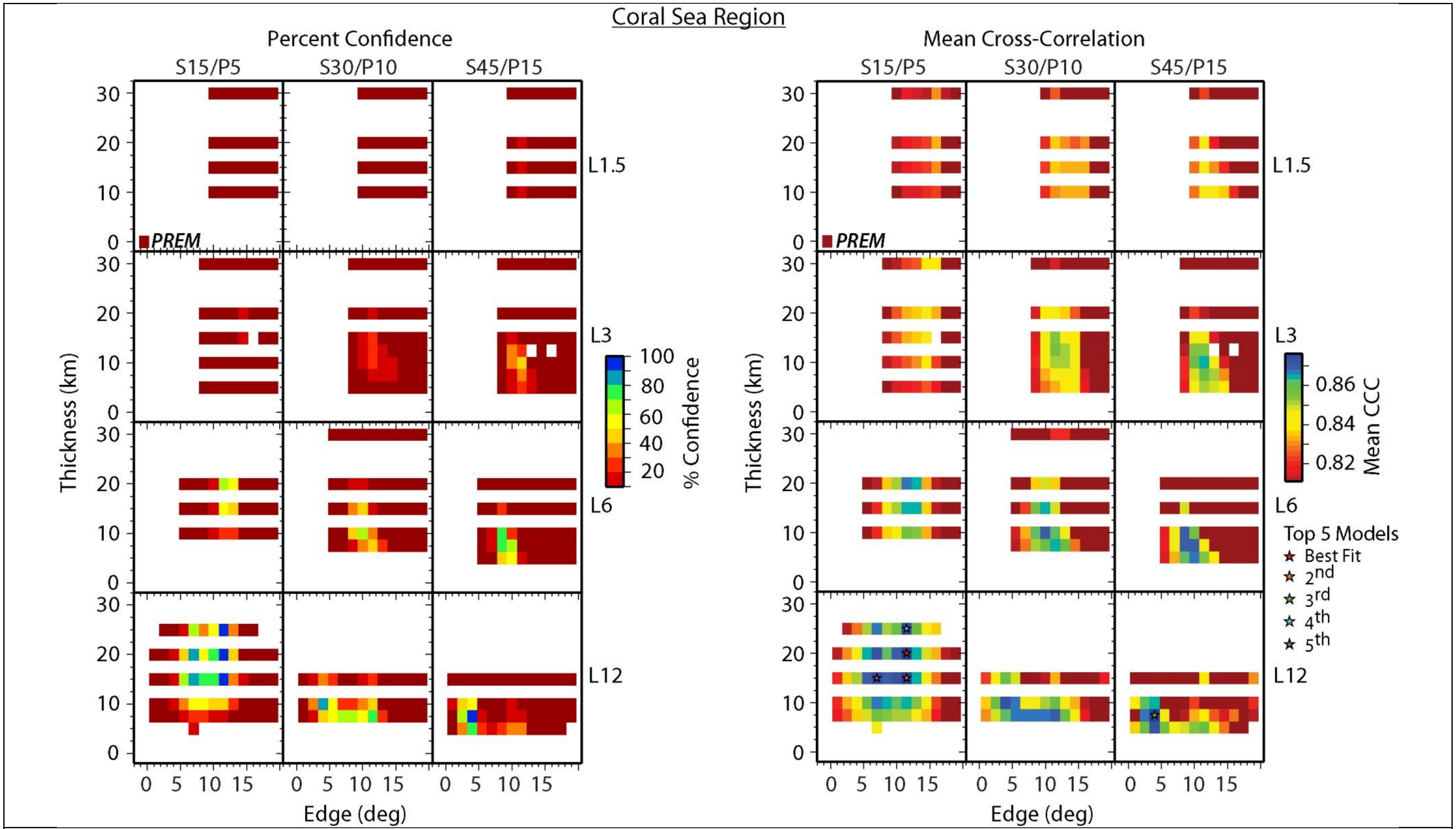

Coral Sea. Bin 1.

South Philippine Sea Region

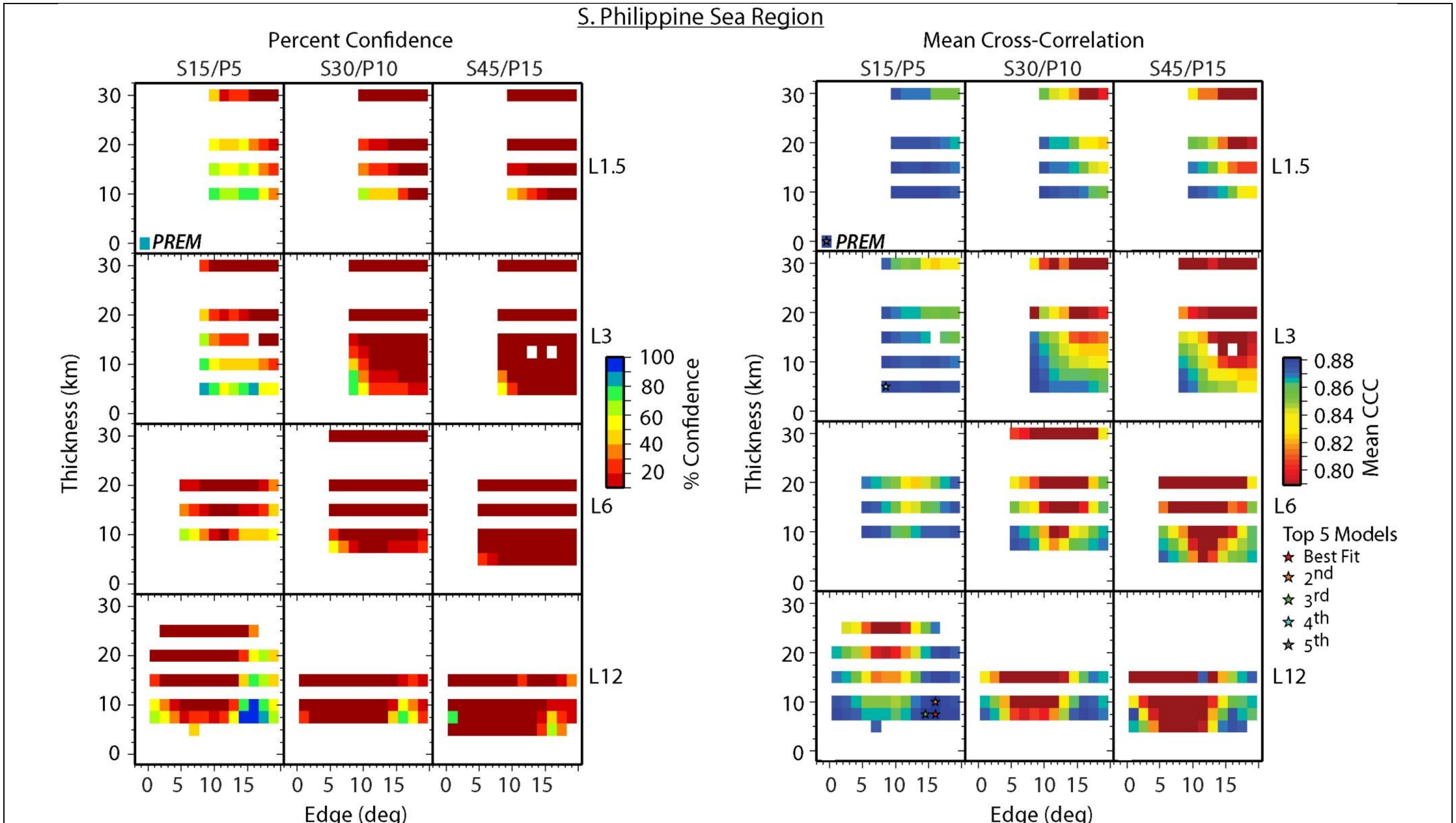

South Philippine Sea. Bin 1.

North Philippine Sea Region

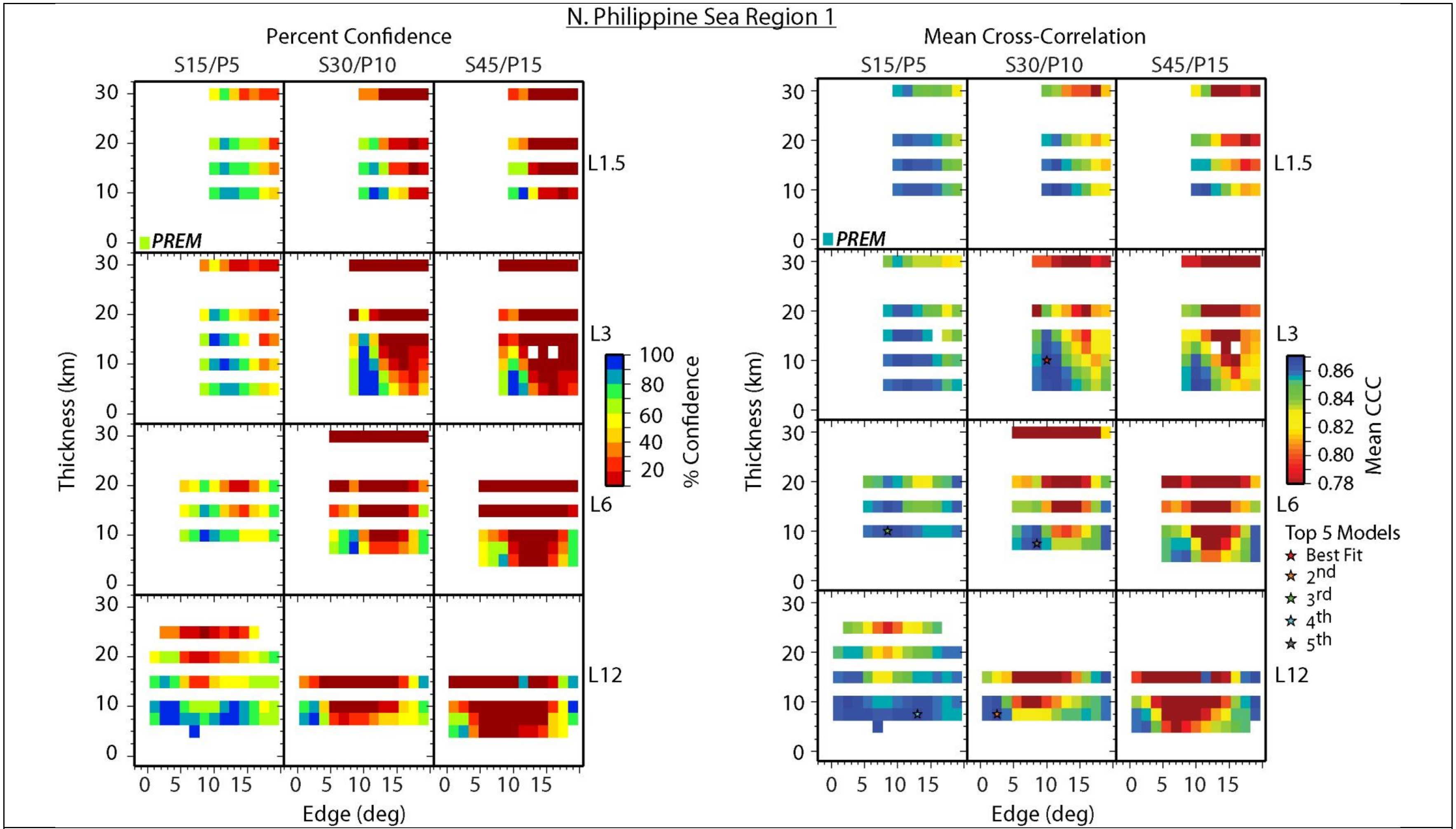

North Philippine Sea. Bin 1.

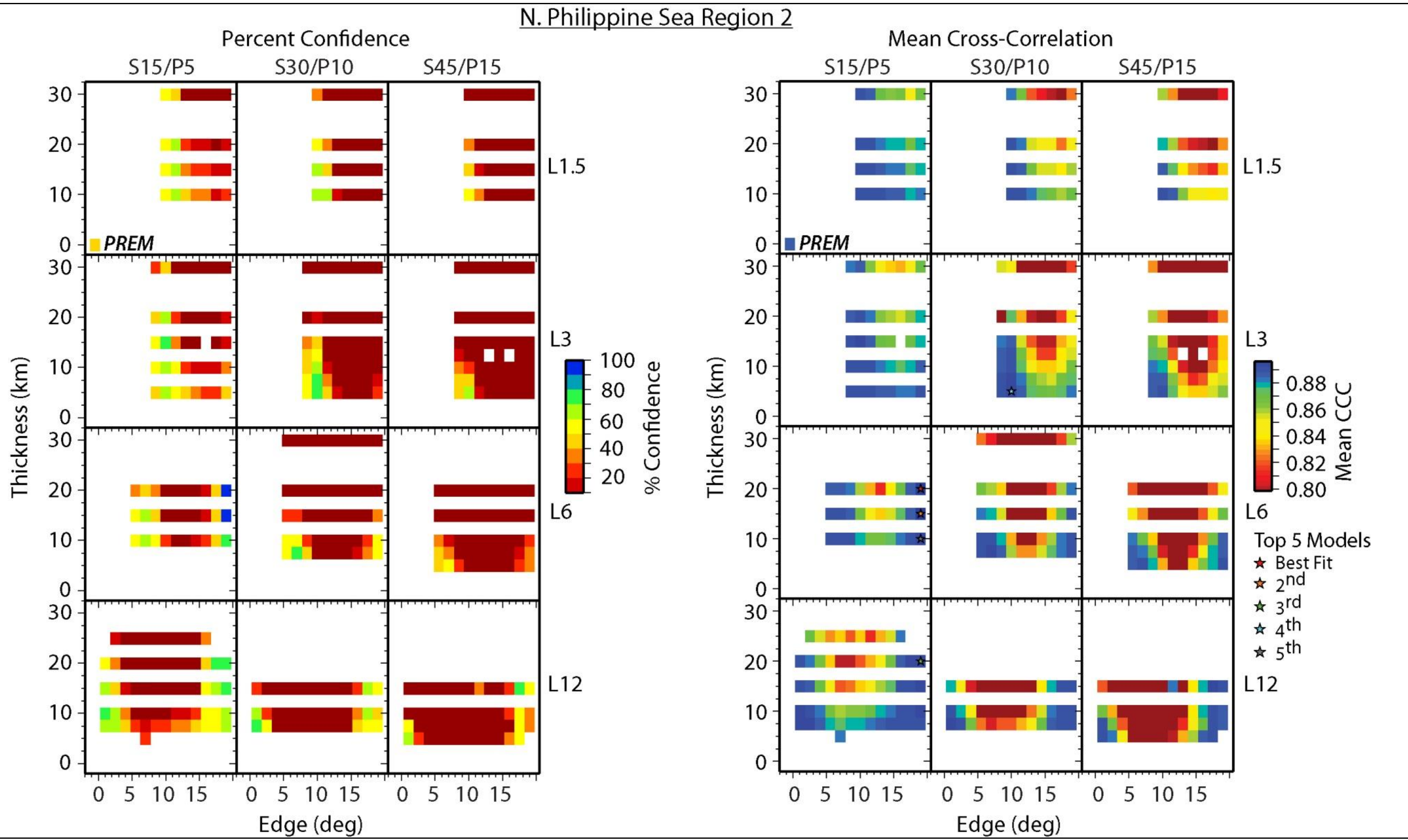

North Philippine Sea. Bin 2.

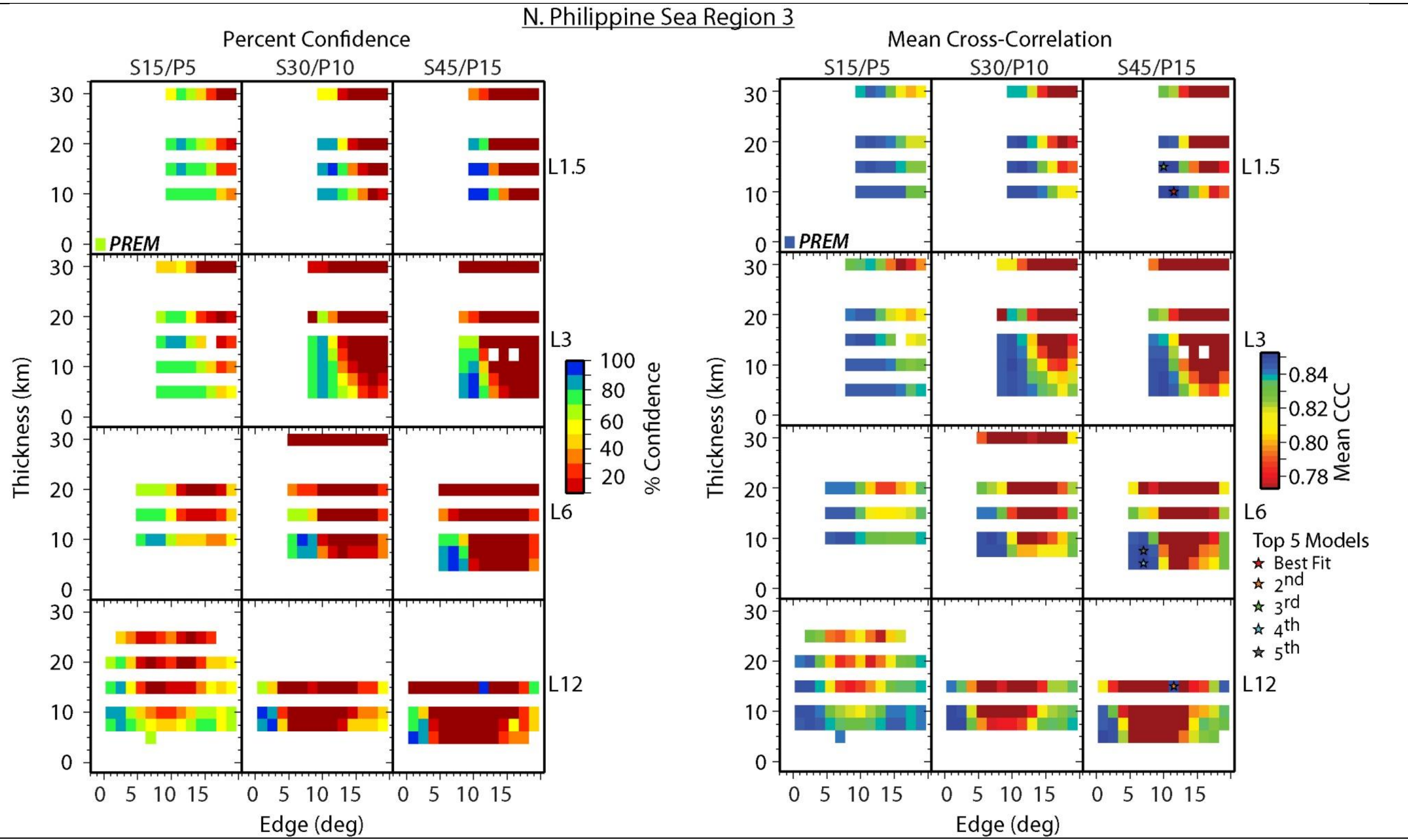

North Philippine Sea. Bin 3.

South China Sea Region

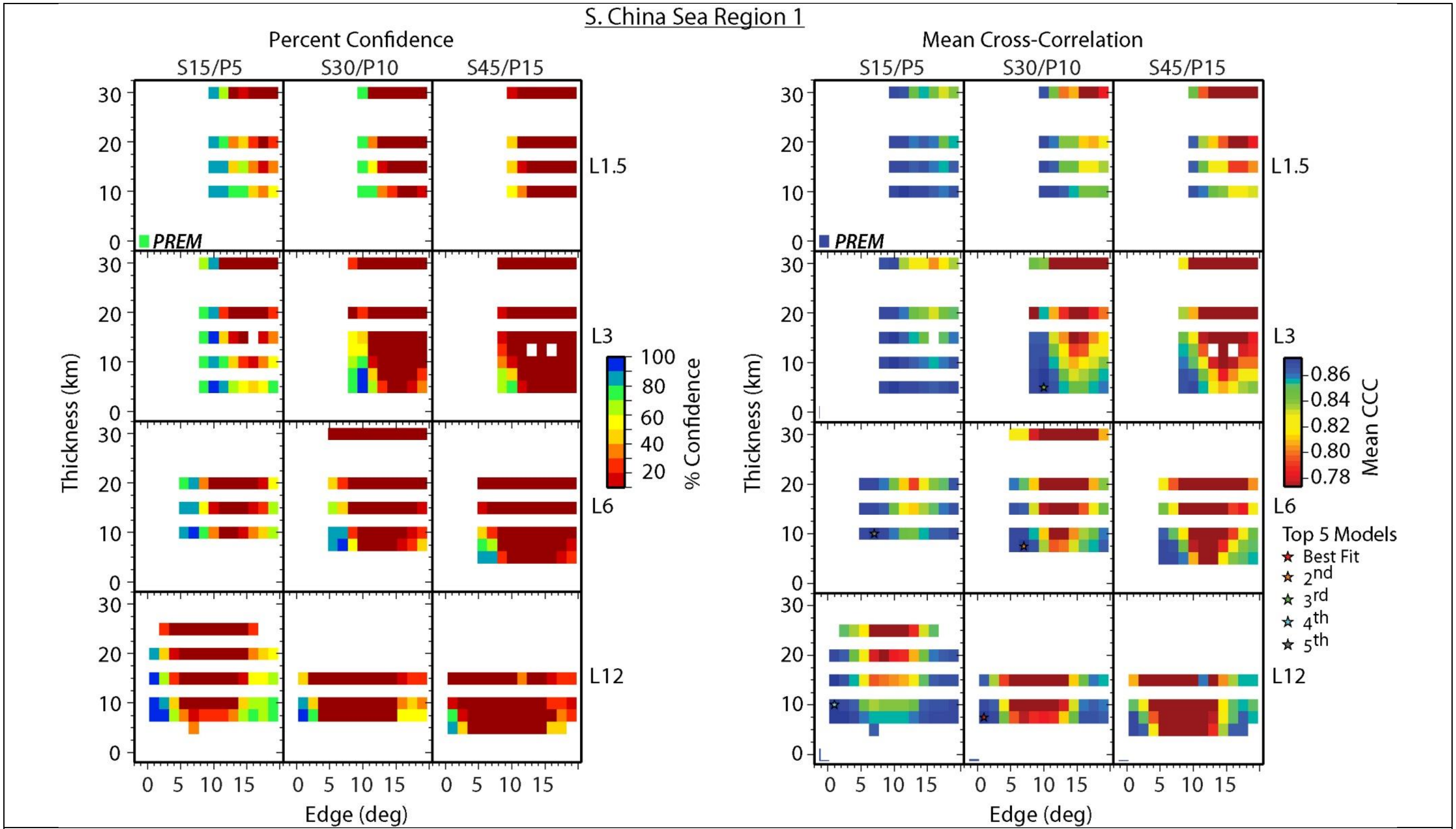

South China Sea. Bin 1.

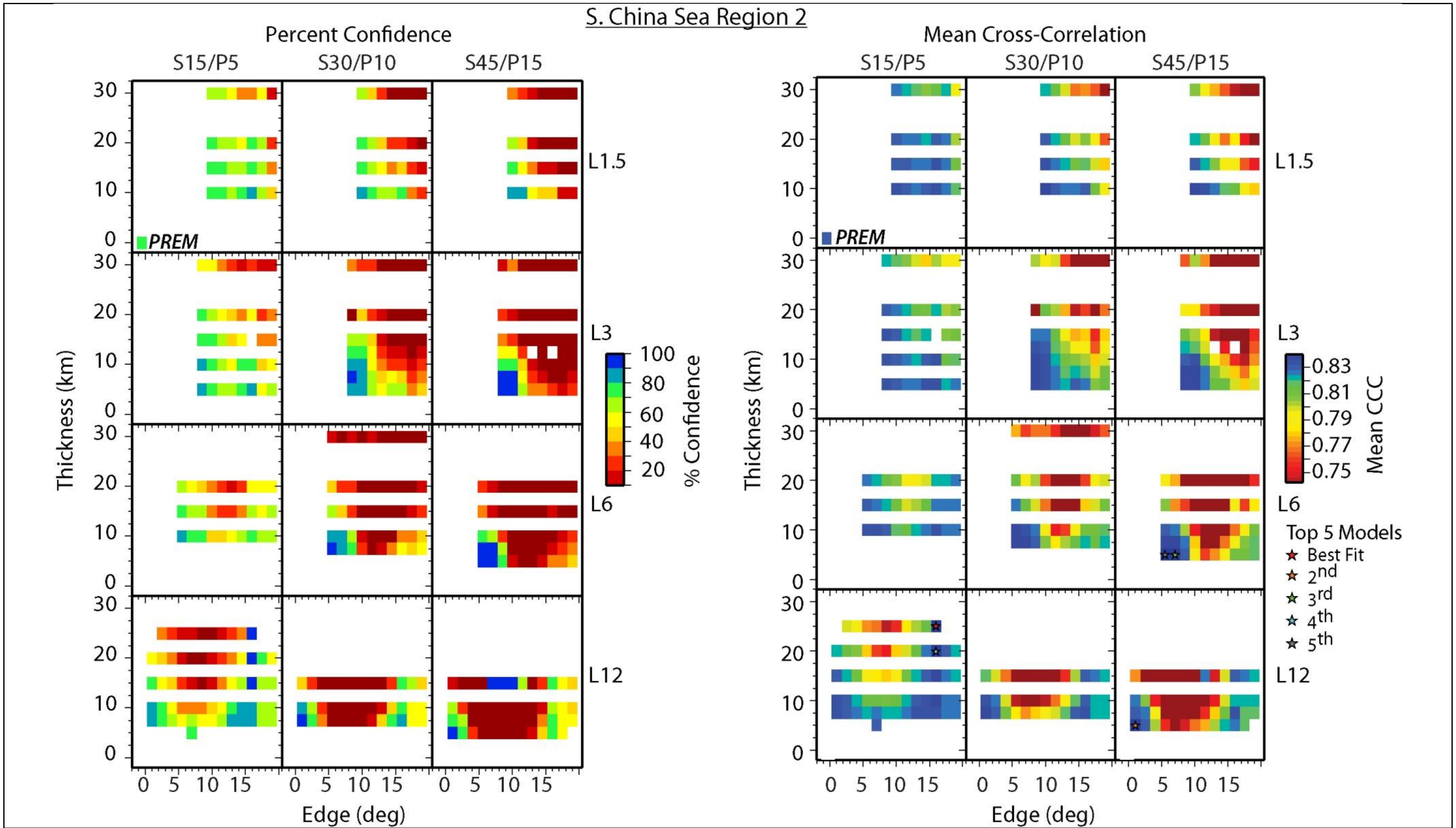

South China Sea. Bin 2.

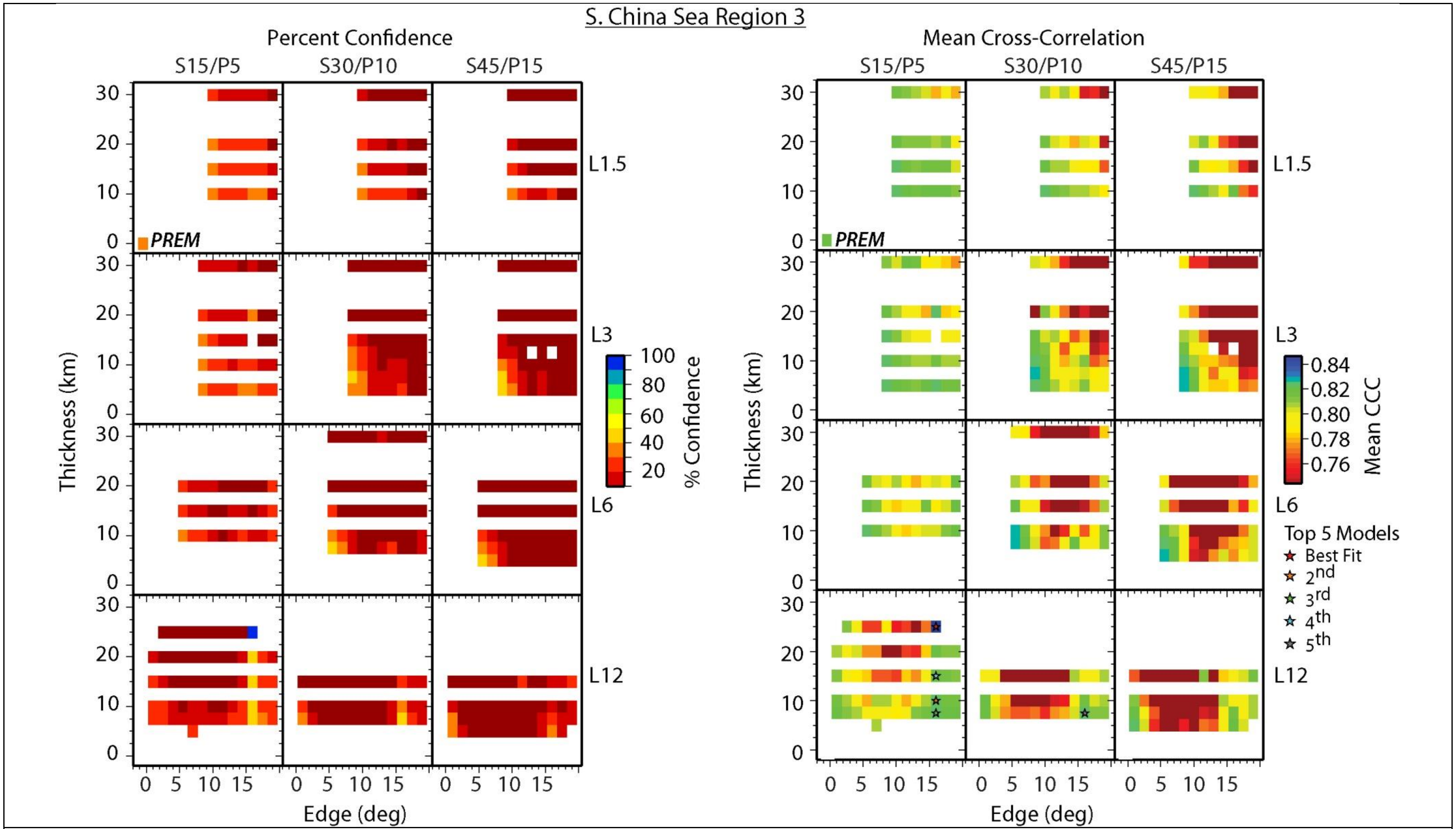

South China Sea. Bin 3.